Online Recording the Position and Orientation of an End-Effector of a Spatial Cable-Suspended Robot for Close Loop Control Using HybridSensors

M. H. Korayem, S. Khayatzadeh, H. Tourajizadeh, M. Taherifar

Robotic Research Laboratory, Center of Excellence in Experimental Solid Mechanics and Dynamics
School of Mechanical Engineering, Iran University of Science and Technology Tehran, Iran
hkorayem@iust.ac.ir

***Abstract*- All of the Degrees of Freedom including of position and orientation of the end-effector of a spatial cable robot are sensed and recorded with a new sensor fusion method in this paper for being used as feedback. This goal is achieved by employing a hybrid methodology of image processing and distance measurement device. The advantage of the proposed algorithm over encoder solution is its higher accuracy for the cases in which the model suffers from structural uncertainties. Moreover, contrary to other end-effector's pose measurement devices, this method is able to record all of 6 spatial degrees of freedom in all of environmental conditions and in whole of the workspace of the robot. Both of camera and lasers are calibrated individually to provide an actual data set. The camera is responsible for observing the planar movement of the end-effector while the lasers provide the altitude and rotation data of the end-effector. The final reported data of position and orientation of the end-effector are evaluated eventually by the aid of both the data of the lasers and camera using a perspective based methodology and presented data fusion formulation. The reported position of the end-effector which is captured in an online way is then employed as feedback for the control center of the robot. By using a closed loop way which is based on feedback linearization algorithm, this center controls the end-effector. A simulation study is done on the ICaSbot (IUST Cable Suspended Robot) which is a spatial cable robot with six DOFs using six actuators. The efficiency of the proposed algorithm is proved by comparing the experimental tests conducted on ICaSbot with the related simulation results which are performed in the MATLAB environment. The tests include statistical analysis of accuracy and repeatability and also dynamic movement of tracking and point to point motion.**

Keywords- Component; Cable Suspended Robot; Feedback Control; Hybrid Sensor Technology; Image Processing; Laser Sensor

I. INTRODUCTION

Cable suspended robot is a type of parallel mechanisms which has closed-loop and under constrained structure. Cable robots are divided into two groups: fully-constrained cable robots and under constrained cable robots [1-2]. By the advent of NIST (National Institute of Standards and Technology) Robocrane, this kind of robots had been developed by many research teams from a planar robot to a six DOFs cable suspended one [3-6]. But the typical cranes have the problem of stability due to their lack of controlling the orientation of the suspended object. This kind of under constrained parallel mechanisms which are considered in this paper provide a practical mechanism for handling and positioning heavy loads while a larger useful workspace can be covered. For controlling this kind of robots, we should obtain the position and orientation of the end-effector and then use them as the actual feedback to control the robot in a closed loop approach. Thus controlling the end-effector position using its output feedback is highly appreciated and considerably increases the accuracy of the robot. In previous models of robocranes, the position and orientation of the end-effector were calculated through the direct dynamics of the robot using the encoder data. Potentiometer is another solution of the mentioned problem [7]. These solutions suffer from some disadvantages. For example some unwanted constraints will be involved in the measurement. Also the accuracy of the system will be decreased as a result of parametric uncertainties or external disturbances, e.g. wind, mechanicals vibration. In this paper a new method of direct measurement of the translational and orientation of the end-effector is proposed which is the result of combination of sensors. Some researchers have been performed in this area so far.

Lee et al. [8] explored a combination of applying vision machine and global positioning system (GPS) technology in developing a robotic crane. But there are some disadvantages in applying GPS unit. The error is about several centimeters so the measurement is not quietly precise. Also, this tool is very expensive. Ottaviano [9] used ultrasonic sensor for a 4 cable-based structure. But when the ultrasonic sensor is used, echoes from walls may cause problems, particularly if the enclosed perimeter is much smaller than the maximum range of the system. This phenomenon is called small room syndrome. Also the reflection of the sound from any obstacles which are located in workspace increases the final error. Mej´ıas et al. used vision system to find the safe landing of a 3 DOFs, 4 cable array robot [10]. In bi-vision method, two cameras are used for locating the position of the end-effector. The main disadvantages of this method is the existence of blind areas (the areas in which at least one of the cameras cannot observe at least one of the markers) since we have several cables, linked to the end-effector which occupy the view of the cameras. Kim and Song [11] had reviewed the potentiality of ultra-sonic, laser, potentiometer and encoder technologies for being used in robotic tower cranes. Lee et al. had studied the efficiency of a combination of laser device, encoder, and accelerometer on controlling system of a robotic tower-crane. Laser devices were used to measure the linear distance while the encoder and accelerometer were used to measure the horizontal and vertical angles [12]. When accelerometer is used, the position and orientation of a point is achieved by two times integration of the axial and rotational acceleration. Finally a single laser cannot be also

employed for complete measurement of position and orientation of an end-effector. The reason is attributed to the fact that by rotating the end-effector the data of the laser is not valid anymore.

However something has not been done yet which is necessary to be considered. In order to overcome the mentioned deficiencies, a new sensor fusion method, is proposed in this paper using 3 laser sensors and one camera to record all the six DOFs of the end-effector of a cable robot in an online way. This record is possible through whole the workspace of the robot in an accurate closed loop way which is applicable in every environmental situation. In this method, three markers are placed on top of the end-effector. A camera is employed for obtaining the roll angle and the planar position of these points. Pitch and Yaw angles together with the height of the end-effector are calculated by three laser sensors which are placed under the end-effector aiming the ground. The online combination of the data of all of the mentioned sensors needs to be employed by the aid of presented data fusion formulation and calibration of this paper in order to evaluate the final actual DOFs of the end-effector and use them in closed loop control of the robot to increase its accuracy. The novelty of the proposed sensing device can be stated as below: Capability of online record of all of DOFs (including of rotational and translational) of the end-effector of a cable robot, Fast calculation possibility which makes it suitable for real-time and closed loop applications, Least environmental limitations which makes it possible to be employed in every industrial places with any dimensional size, covering whole the workspace of the cable robot.

The cable robot formulation including of dynamics and its control based on feedback linearization method are explained in Section 2. Section 3 introduces sensor installation and procedure of using the sensor data as the feedback of close loop controller of the robot. In Section 4 camera and lasers calibration is performed. Finally the efficiency of this new method is verified in Section 5 by comparing the experimental tests which are conducted on IUST cable robot called ICaSbot with simulation results of MATLAB software. Also the experimental results of controlling method using this novel feedback system are compared with the results of joint space control algorithm which uses just encoders to control the motors. The accuracy and repeatability of the robot is proved by providing statistical analysis and the superiority of the proposed recording device and designed controller is shown by conducting both of tracking and point to point motions.

II. CONTROL STRATEGY

Consider a cable suspended robot which is suspended through six cables and has 6 degrees of freedom as (x,y,ψ,Θ,ϕ) (Fig. 1). By using Newton–Euler eq. we have the following dynamic eq. [13]:

$$D(X)\ddot{X}+C(X,\dot{X})\dot{X}+g(X)=-J^{T}(X)T \tag{1}$$

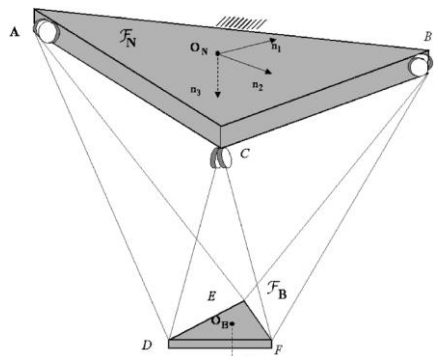

Fig. 1 Schematic of 6 cable robot [14]

Where:

$$D=\begin{bmatrix} mI_3 & 0 \\ 0 & P^{T}IP \end{bmatrix};C=\begin{bmatrix} 0_3 \\ P^{T}\{IP\dot{o}+(P\dot{o})\times I(Po)\} \end{bmatrix};g=\begin{bmatrix} 0 \\ 0 \\ -mg \\ 0_3 \end{bmatrix};$$
$$S=-J=\left[\frac{-\partial q_i}{\partial x_j}\right]_{i\times j};P=\begin{bmatrix} 1 & 0 & -\sin\Theta \\ 0 & \cos\psi & \sin\psi\cos\Theta \\ 0 & -\sin\psi & \cos\psi\cos\Theta \end{bmatrix};\dot{o}=\begin{bmatrix} \dot{\Psi} \\ \dot{\Theta} \\ \dot{\phi} \end{bmatrix} \tag{2}$$

T is the vector of cables tension, $D(x)$ is the inertia matrix, $C(x,\dot{x})$ is the vector of velocity terms, $g(x)$ is the gravity vector, J is the conventional parallel manipulator Jacobian, X is the vector of DOFs of the system, m is the mass of the end-effector, I is the moment of inertia of the end-effector and q is the length of the cables. Also the dynamics of the motor is as follow:

$$T=\frac{1}{r}\left[\tau-j\left(\frac{d}{dt}\left(\frac{\partial\beta}{\partial X}\right)\dot{X}+\frac{\partial\beta}{\partial X}\ddot{X}\right)-c\frac{\partial\beta}{\partial X}\dot{X}\right] \tag{3}$$

where J is the matrix of rotary inertia of the motors, c is the viscous friction matrix of the motors, $\dot{\beta}$ is the vector of angular velocity of the motors and τ is the vector of motors torque. By coupling these two dynamics, we have:

$$D(X)\ddot{X}+C(X,\dot{X})\dot{X}+g(X)= -J^{T}(X)\frac{1}{r}\left[\tau-j\left(\frac{d}{dt}\left(\frac{\partial\beta}{\partial X}\right)\dot{X}+\frac{\partial\beta}{\partial X}\ddot{X}\right)-c\frac{\partial\beta}{\partial X}\dot{X}\right] \tag{4}$$

By considering 6 degrees of freedom for cable suspended robot, state space can be developed as below [14]:

$$\begin{cases} z_1=x;z_2=\dot{x};z_3=y \\ z_4=\dot{y};z_5=z;z_6=\dot{z} \\ z_7=\psi;z_8=\dot{\psi};z_9=\theta \\ z_{10}=\dot{\theta};z_{11}=\varphi;z_{12}=\dot{\varphi} \end{cases} \Rightarrow \begin{cases} \dot{z}_i=z_{(i+1)};if:i=odd;i=1,...,12 \\ \dot{z}_i=\frac{1}{D}(-C\dot{X}-g+S^{T}T)_{i/2};if:else \end{cases} \tag{5}$$

Based on feedback linearization torque can be calculated as below:

$$T_i = \{ S^{-T}(D\nu + C\dot{X} + g)\}_i \Rightarrow$$
$$\tau_i = rS^{-T}(D\nu + C\dot{X} + g) + J\ddot{\beta} + C\dot{\beta}; i = 1,.,6 \quad (6)$$

In which, ν can be substituted as below based on feedback linearization method:

$$\nu_i = \ddot{z}_{(2i-1)d} + K_{iD}(\dot{z}_{(2i-1)d} - \dot{z}_{(2i-1)})$$
$$+K_{iP}(z_{(2i-1)d} - z_{(2i-1)}); i = 1,.,6 \quad (7)$$

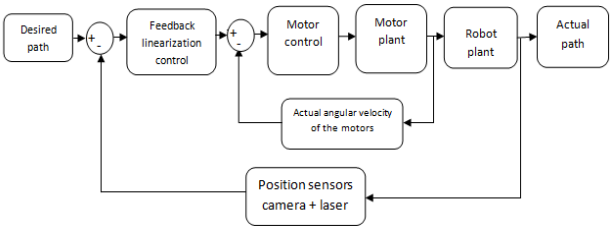

Fig. 2 Control procedure of the robot based on feedback linearization [14]

To sum up, a combination of position sensors including of camera and lasers is employed in order to monitor and feedback the online data of end-effector's DOFs. The lasers are responsible of recording the altitude of the end-effector together with its angles while the camera is used to monitor its planar movement (Fig. 3). Generally the overall scheme of the close loop controlling system of the robot is depicted in Fig. 2. It can be seen that two sequential closed loop controller are involved here including of motor controller and end-effector controller. The angular velocity of the motors is controlled using encoder sensor each 0.01 seconds in the inner loop of robot cable while the position of the end-effector are controlled each 0.1 seconds using the position feedback which is provided in an online way based on the proposed algorithm of this paper.

III. SENSOR INSTALATON

As described before, using encoder data is a way to monitor the actual pose (position and orientation) of the end-effector. However this method is not completely reliable while any kind of parametric uncertainties including of clearance of the motors, flexibility of the cables and etc. makes considerable error in the results. In order to reduce the effect of these uncertainties a new method that provides the actual position and orientation of the end-effector in an online way using a proper pose sensor is employed. This goal is achieved by the aid of mixed algorithm combined of using lasers and image processing which is proposed in this paper. This method uses for monitoring the actual position and orientation of the end-effector of the ICaSbot cable robot. The camera is responsible of gathering the planar movement of the end-effector while the lasers provide the altitude and rotation data of the end-effector. So by the aid of three lasers which are installed at the bottom of the end-effector which provides a pyramid shape geometry under the end-effector, the altitude and orientation of the end-effector can be easily calculated using the Eqs. (8, 12-15). Afterward by importing the filtered data of the lasers to the camera, real planar coordinate of the end-effector is obtained by the aid of Eq. (16). This procedure is required to be performed for three tips of the end-effector's triangle to cover all of the DOFs of the end-effector.

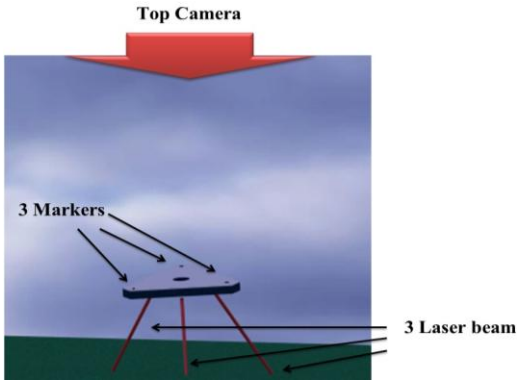

Fig. 3 Strategy of recording all of end-effectors DOFs by coupling the camera and laser data

In order to obtain and process the sensors and camera data and use them for controlling the robot two linked PCs are employed. The analyzed data of image processing and also lasers which have processed in MATLAB environment should transfer into the LabVIEW environment which whole the graphical user interface and simulator of the cable robot is designed there. But providing the controlling and timing consistency of two software packages (MATLAB and LabVIEW) is not possible by the aid of a single PC. So two PCs are employed here by which the second one analyses the image processing of the camera data (MATLAB) while the first one is responsible of processing the data related to the lasers and also dynamics and control of the robot in an online way. Following chart in Fig. 4 shows the methodology of online timing that was required to provide the consistency of two PCs.

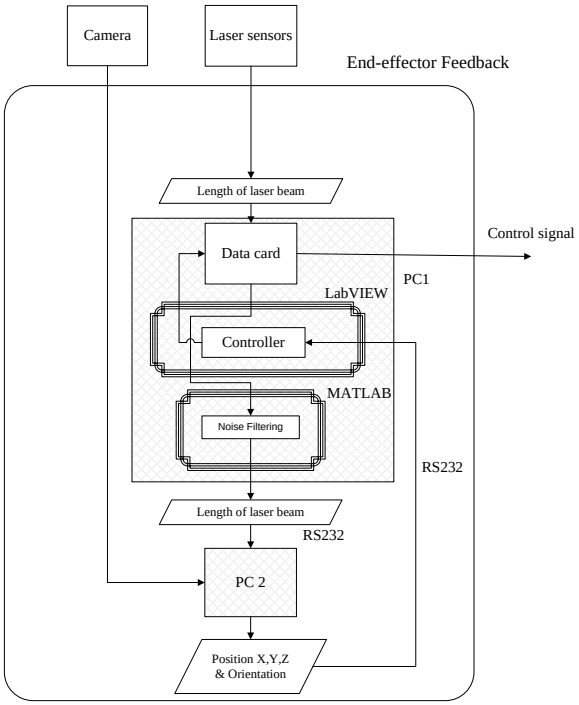

Fig. 4 Flowchart of information architecture

It is noteworthy that PC1is employed for controlling the robot and PC2 is responsible of analyzing the camera and calculate the real pose of the end-effector. First of all the data related to the lasers are received by the PC1 through the digital data card (The data card which is used for reading the

data of loadcells and laser sensors is "Advantech-PCI-1711L). Then the data are transferred to the second PC by the aid of serial port and RS232 protocol. Then the actual position of the end-effector is evaluated in PC2 using image processing together with the altitude of the end-effector which is provided by the aid of lasers. Finally the obtained data will be then transferred into the PC1 by the aid of the same serial protocol to be used as the end-effector feedback in controlling the robot.

A. Image Processing

The software setup of the image processing is programmed in MATLAB and the steps of initial image processing are shown in Fig. 5. After running initial process, all objects which are similar to circle with a medium range of diameter are distinguished and pointed by a red star (Fig. 5). In the second step, the operator is asked to select the three markers by right-clicking of the mouse. In that case, our main three markers are presented to the software and thus the software starts recording the data. According to the high volume of processing and the time-delay related to that, we crop the image of the camera to decrease the volume of the processing. This kind of cropping is conducted for the areas near our three markers.

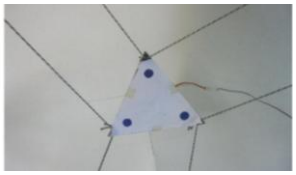

Fig. 5a

Fig. 5b

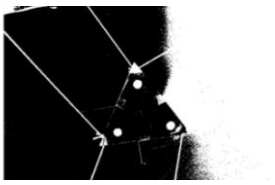

Fig. 5c

Fig. 5d

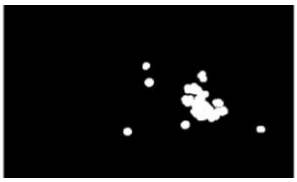

Fig. 5e

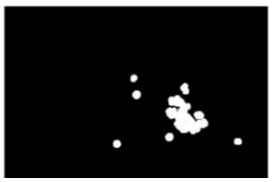

Fig. 5f

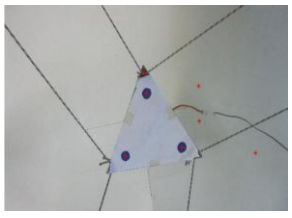

Fig. 5g

Fig. 5 Initial image processing

One sample of image processing is shown in Fig. 6. According to the presented sensor installation, it is obvious that this proposed sensor fusion device can be easily installed in every environmental situation, since there is no bug in the employed sensors. Also there is no limitation for covering whole the workspace of the robot, since the camera is wide and sensors are able to cover an acceptable range.

B. Pose Calculation

By installing three lasers through three tips of the end-effector with a specific angle, the laser lines configure a half pyramid. So the geometry of the pyramid and then the altitude of end-effector in *z* direction will be known completely by the aid of following formulation:

Fig. 6a

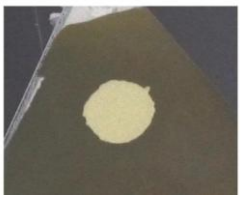

Fig. 6b

Fig. 6c

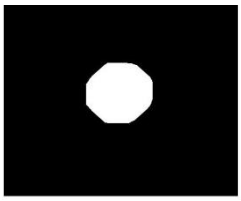

Fig. 6d

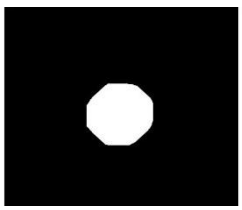

Fig. 6e

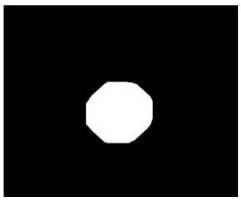

Fig. 6f

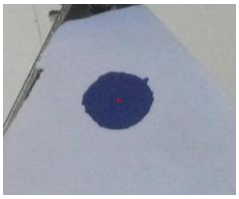

Fig. 6g

Fig. 6 Image processing (using cropping technique)

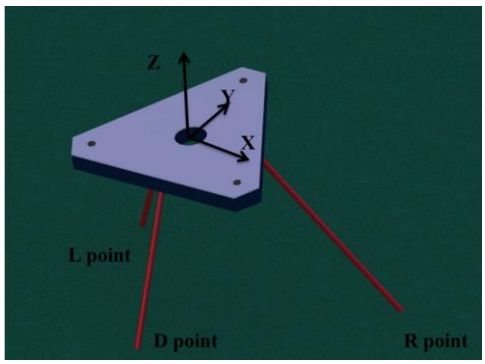

Fig. 7 Local coordinate placed on the centroid of the end-effector

Considering 60 degrees angle for each laser, the lengths of edges $L_R; L_U; L_L$ are obtained. A local coordinate is set in the centroid of the end-effector and the local *X, Y, Z* of the points of intersection of the lasers with the ground can be calculated by knowing the angle of the lasers respect to the vertical axis (Fig. 7).

$$
\begin{aligned}
x_R &= (0.5L_R + {}^{d}/_{2\sqrt{3}})\cos 30 \\
y_R &= (0.5L_R + {}^{d}/_{2\sqrt{3}})\sin 30 \\
z_R &= -0.5\sqrt{3}L_R \\
x_L &= -(0.5L_R + {}^{d}/_{2\sqrt{3}})\cos 30 \\
y_L &= (0.5L_R + {}^{d}/_{2\sqrt{3}})\sin 30 \\
z_L &= -0.5\sqrt{3}L_R \\
x_D &= 0 \\
y_D &= {}^{-d}/_{2\sqrt{3}} \\
z_L &= -0.5\sqrt{3}L_R
\end{aligned}
\tag{8}
$$

where *d* is the length of the end-effector triangle edge. Calculating the local coordinate of three mentioned intersection points, the eq. of the plane which includes these three points can be calculated:

$$a(x-x_0)+b(y-y_0)+c(z-z_0)=0 \tag{9}$$

where a, b and c are the resultant vectors of cross products of $RL \times RU$ and *x0*, *y0*, *z0* are the local coordinate of one of the tips. Now by substituting the local *x* & *y* of each tips in this plane formula the vertical distance of each tip respect to the end-effector angle can be easily calculated which is called z. Finally the vertical altitude of each tip from the ground (*h*) can be extracted by multiplying this distance by $\cos\gamma$.

$$h = z\cos(\gamma);\cos\gamma = \frac{c}{\sqrt{a^2+b^2+c^2}} \tag{10}$$

where γ is the angle of normal vector of the end-effector compared to vertical axis. Now the scaling of the image processing can be completed by knowing the altitude of each tip of the end-effector. The real coordinate of each tip can be obtained by the aid of the raw data of the camera together with the resultant altitude of each tip. Finally the coordinate of the end-effector centroid can be evaluated by the aid of the real calculated coordinate of three tips of the end-effector:

$$
\begin{aligned}
x_G = \frac{X_R + X_L + X_U}{3}, y_G = \frac{Y_R + Y_L + Y_U}{3} \\
and\ \ z_G = \frac{Z_R + Z_L + Z_U}{3}
\end{aligned}
\tag{11}
$$

Alternatively the global angles of the end-effector can be calculated using Eqs. (13-15) and the following formulations:

$$
\begin{aligned}
A &= \frac{a}{\sqrt{a^2+b^2+c^2}} \\
B &= \frac{b}{\sqrt{a^2+b^2+c^2}} \\
C &= \frac{c}{\sqrt{a^2+b^2+c^2}}
\end{aligned}
\tag{12}
$$

So the angles of the end-effector can be calculated as below:

$$Yaw = \tan^{-1}(\frac{A}{-B}) \tag{13}$$

$$Pitch = \frac{\sqrt{A^2+B^2}}{C} \tag{14}$$

The roll can be obtained by the aid of vision data:

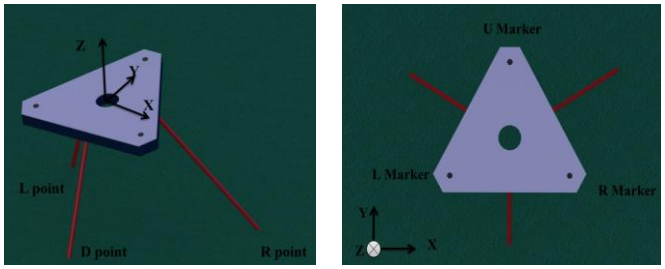

a. b.

Fig. 8a Local coordinate b Global coordinate

Since the Global XY-coordination of three markers are known by the use of camera (the Global coordination of *U*-marker: (X_U, Y_U) and also for R-marker and *L*-marker: (X_R, Y_R) & (X_L, Y_L) we can evaluate Roll by the aid of following eq. (Fig. 8):

$$Roll = \tan^{-1}(\frac{Y_R - Y_L}{X_R - X_L}) \tag{15}$$

While the robot is moving, the data of *X*, *Y* and *Z* position and three axial orientations is recorded in a matrix in MATLAB's workspace to be used as feedback control for each time step. So it can be seen that based on the proposed method all of the DOFs of the robot including of translational and rotational can be exactly evaluated. Also there is no need for high calculation which makes it possible to be used in a real-time way and thus closed loop control of the robot is possible in an online way in order to increase the accuracy of the robot.

IV. CALIBRATION

A. Camera

As it was discussed before, the camera which is installed at the top of the robot and observes the end-effector, records the raw data of planar coordinate of the end-effector. Raw data means that the recorded data needs two steps of calibration.

Data fusion is used here for combining the data of the lasers and camera. In order to find out the real value of altitude and orientation of the end-effector, the data of the lasers are required to calibrate the perspective of the camera. The first step of calibrating which is known as planar calibration is conducted just one time after installing the camera on the robot. Perspective calibration which is the second step of calibrating should be renewed for every data.

By using a chess shape plate for planar calibration, we specify two points for which their real planar coordinate is known. At the start of running the program, three markers should be selected by clicking on the picture of the first shot of the camera. Then the program starts converting the raw

data of the positions of three markers which were selected manually by using perspective calibration (Fig. 9).

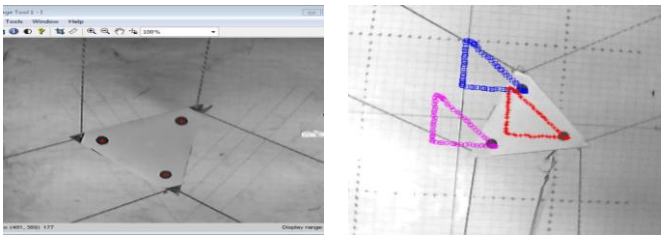

Fig. 9 Image preprocessing, Image processing

Perspective calibration is needed since we have perspective effect while we record image by a camera (Fig. 10).

$$X_{real} = \frac{X_{raw} \times (h + f)}{f} \tag{16}$$

Eq. 16 is used for perspective calibrating. In which f is a physical parameter and should be obtained by an experiment which will be discussed later and h is the distance between the object and the lens of the camera and varies by changing the height of the camera, so we should renew this eq. for every data by using the height of the last data.

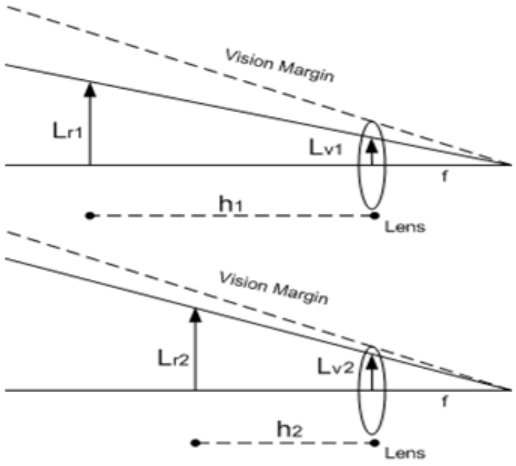

Fig. 10 The scheme of the reflection of the object on the lens of the camera (perspective effect)

For calculating the f parameter, we place an object which has a specific length in front of the camera in two different distances, *h1 & h2*. By substituting the obtained lengths of the object of raw data, L_{V1} and L_{V2}, in Eq. 17 we obtain the *f* parameter.

$$\begin{cases} \frac{L_{V1}}{f} = \frac{L_{r1}}{h_1 + f} \\ \frac{L_{V2}}{f} = \frac{L_{r2}}{h_2 + f} \end{cases} \tag{17}$$

B. Lasers

"GP2D12" is chosen as the distance measuring laser sensor. In this kind of sensors, sensor has light emitter and receiver. The light receiver unit receives a specific light frequency which is emitted by light emitter unit toward the object. Three laser sensors are installed under the end-effector facing the ground (Fig. 11).

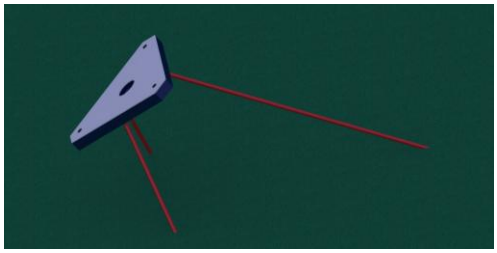

Fig. 11 Symbolic scheme of laser beam

In this research, sensors are calibrated again, since we observed that the sensors do not comply with the calibration function of their catalogue (Fig. 12).

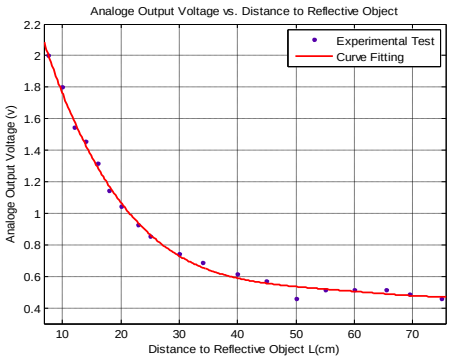

a.

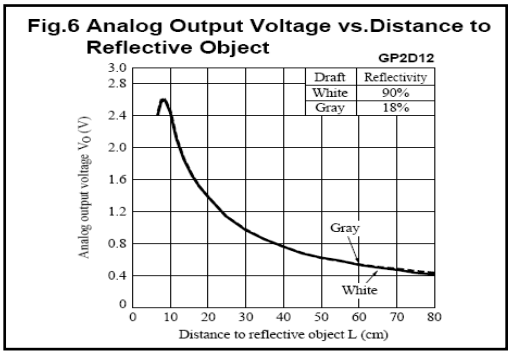

b.

Fig. 12 Calibration test related to laser sensor, a. Experiment data, b. Catalog data

V. TESTS AND RESULTS

In this section an experimental study is conducted on the Iran University of Science and Technology cable robot (ICaSbot) which is an under constrained cable robot supporting 6 DOFs using 6 actuating cables and 6 DC motors (Fig. 13) [15]. The tests are compared and analyzed with the simulation results in order to verify the efficiency and accuracy of the proposed measurement of end-effector position and validate the employed controlling strategy. First, pose accuracy and repeatability are measured according to the ISO tests. The experimental results of end-effector path are extracted using two different strategies. In the first approach the path is tracked in an open loop way using the encoders' feedback (joint space control methodology). The second approach employs the actual position of the end-

effector by the aid of proposed methodology of the present paper and uses it as the controlling feedback of the end-effector to improve the trajectory (Cartesian space control). It is shown here by the aid of two categories of comparative experiments that the second proposed approach provides considerably more accurate results since the external disturbances and parametric uncertainties can be easily neutralized by the aid of measured actual position and orientation of the end-effector. The first comparison is related to tracking case in which the end-effector should track a predefined trajectory which is a triangle here. For the second comparison a regulation scenario is provided in which the robot is supposed to track an optimal path between two predefined initial and final points. The efficiency of the proposed closed loop controlling strategy is investigated and compared for these two scenarios.

TABLE I GEOMETRICAL SPECIFICATION OF THE ROBOT AND MOTOR

Body	
Height	120 cm
Variable side length of base triangle	100-120 cm
Weight	350 kg
End Effector	
Side length of base	17 cm
Thickness	8 mm
Weight	1100 g

Motor	
mark	DC gear motor
model	Buehler 1.61.070
Reference voltage	12 v
No Load Speed	103 rpm
max Torque	910 mN.m
rated Current	1.4 A
reduction ratio	1:25.2
Weight	220 g

Fig. 13 Scheme of the designed IUST cable robot [15]

A. Pose Accuracy and Pose Repeatability

In order to verify the efficiency of the recording and controlling method from the statistical analysis point of view, pose accuracy and pose repeatability are measured using ISO9283 [16].

1) Accuracy of Positioning:

For 10 cycles in the same direction with a 1.100 kg load on the end-effector, this measurement is done. To meet this goal it is needed to conduct a tracking movement from a definite point toward a desired goal like z_c, y_c, x_c for n times and record its actual destination (z_j, y_j, x_j). So accuracy of positioning based on this ISO can be written as:

$$\begin{aligned} AP_P &= \sqrt{(\bar{x}-x_c)^2+(\bar{y}-y_c)^2+(\bar{z}-z_c)^2} \\ AP_x &= (\bar{x}-x_c) \\ AP_y &= (\bar{y}-y_c) \\ AP_z &= (\bar{z}-z_c) \end{aligned} \tag{18}$$

The mean value of the recorded coordinates related to n times tests are $\bar{z}, \bar{y}, \bar{x}$. so:

$$\bar{x} = \frac{1}{n}\sum_{J=1}^{n} x_j \,,\ \bar{y} = \frac{1}{n}\sum_{J=1}^{n} y_j \,,\ \bar{z} = \frac{1}{n}\sum_{J=1}^{n} z_j \tag{19}$$

Based on this procedure following results are gained. The desired set points are set as Table (2) and the actual end points of the tracked end-effector for each test are seen as Table (3).

TABLE II SET POINT OF ISO TESTS

x_c	y_c	z_c	unit
100	100	800	mm

TABLE III RESULTED POINTS OF ISO TESTS

No.	x_j	y_j	z_j	unit
1	103.8	93.5	763.5	mm
2	102.3	96.7	675	mm
3	104.2	100.9	751.6	mm
4	106.9	100.8	832.7	mm
5	108.9	100.1	832.7	mm
6	111.3	96.9	800.4	mm
7	105.4	81.8	789.6	mm
8	104.1	79.2	862.0	mm
9	105.8	82.7	832.2	mm
10	103.1	86.3	891	mm

By using the mentioned equations the actual mean value is calculated:

TABLE IV ACTUAL MEAN VALUE

$\bar{x}$	$\bar{y}$	$\bar{z}$	unit
105.6	91.9	803	mm

$$\begin{aligned} &AP_P = \sqrt{(105.6-100)^2+(91.9-100)^2+(803-800)^2} \\ &\Rightarrow AP_P = 10.31mm \end{aligned} \tag{20}$$

2) Repeatability of Positioning:

The repeatability is a conventional accuracy of the end point positioning of the end-effector for n times tests and compatibility of the position and orientation of these results. Based on this standard convention positioning repeatability (RPL) is the radius of the sphere like:

$$RP_L = \bar{L} + 3S_L \tag{21}$$

where:

$$\bar{L} = \frac{1}{n}\sum_{j=1}^{n} L_j$$

$$L_j = \sqrt{(x_j-\bar{x})^2+(y_j-\bar{y})^2+(z_j-\bar{z})^2}$$

$$S_L = \sqrt{\frac{\sum_{j=1}^{n}(L_j-\bar{L})^2}{n-1}} \tag{22}$$

According to the mentioned obtained results we have:

$$\bar{L} = 48.6\ ,\ S_L = 36 \Rightarrow RP_L = 156.8 \tag{23}$$

It can be seen that an acceptable accuracy and repeatability can be provided using the presented recording and controlling strategy.

B. Triangle Test

For verifying the precision of the Robot in tracking, a triangle test is conducted for which the end-effector is responsible to track a right-angled triangle trajectory. Eq. of the triangle path:

$$X = 0; Y = 0.1 - \frac{(t-1.64)}{16.4}; Z = 0.9$$
$$0 < t < 1.64 \tag{24-a}$$

$$X = \frac{(t-1.64)}{16.4}; Y = 0; Z = 0.9$$
$$1.64 < t < 3.28 \tag{24-b}$$

$$X = 0.1 - \frac{(t-3.28)}{23.2}; Y = \frac{(t-3.28)}{23.2}; Z = 0.9$$
$$3.28 < t < 5.6 \tag{24-c}$$

The effectiveness of the two different controller systems of the mentioned closed-loop controller is validated by comparing the tracked trajectory of these two systems in Fig. 14 and analyzing their related errors in Fig. 15 (The scales are meter). First of all it can be seen that an acceptable compatibility can be observed between the simulation results and experimental test. Moreover it is obvious that the tracking accuracy of the controlling system equipped by the end-effector feedback is much better than the one equipped by joint space feedback. The comparison of angular velocity of the motors between simulation and experimental results of Cartesian space controller are shown in Fig. 16. The similar trend of simulation and experiment shows the correctness of simulation and also experimental setup of encoders. A little vibration of the experimental results around the simulation profile can be referred to the structural flexibility and friction of the manufactured robot which is not modeled in the simulation and also high resolution of the encoders. In order to have a better evaluation of the accuracy of each system the norm of error of the systems are calculated using the following eq.:

$$E = \sqrt{(x_1 - x_2)^2 + (y_1 - y_2)^2 + (z_1 - z_2)^2} \tag{25}$$

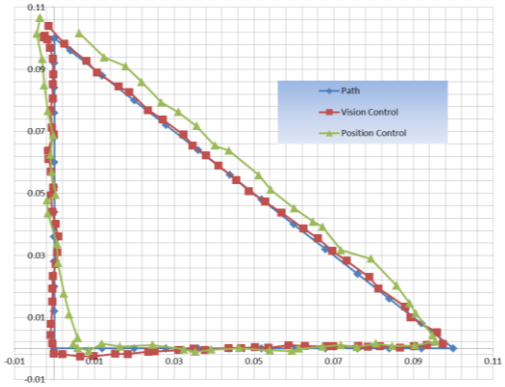

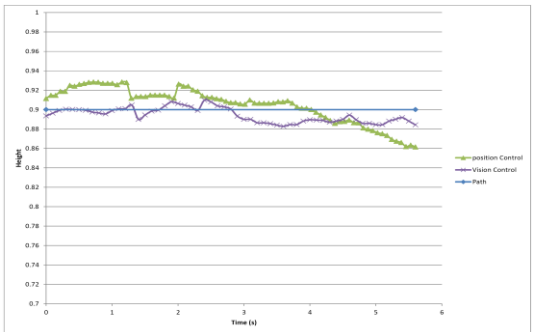

Fig. 14 Comparing the result of simulation path and experiment path of the triangle test

In Eq. (25), x_1, y_1, z_1 is the desired position and x_2, y_2, z_2 is the actual position of the end-effector in trajectory tracking.

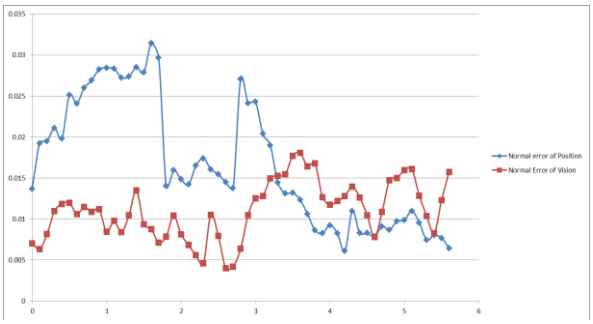

Fig. 15 Error norm of path tracking in triangle test

As we expected the normal error of vision control (about 1 cm) is considerably less than the joint space control (2 cm)

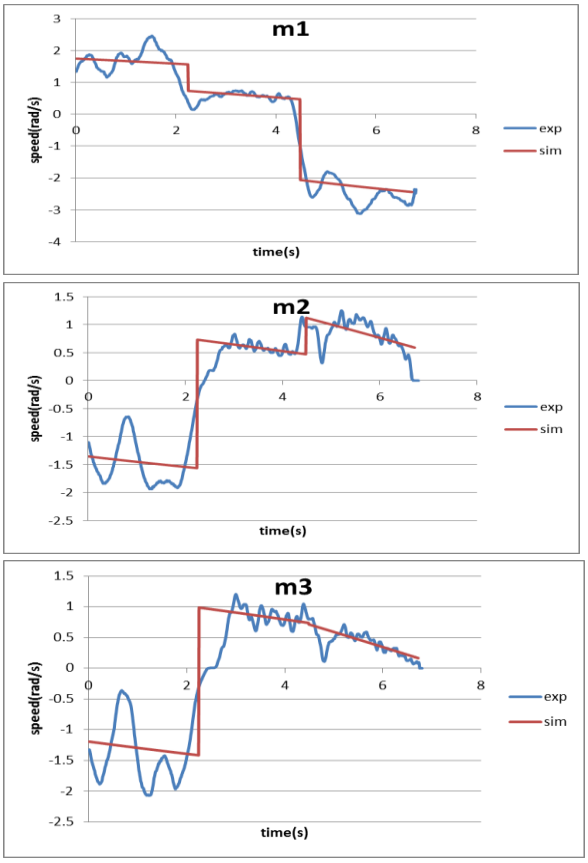

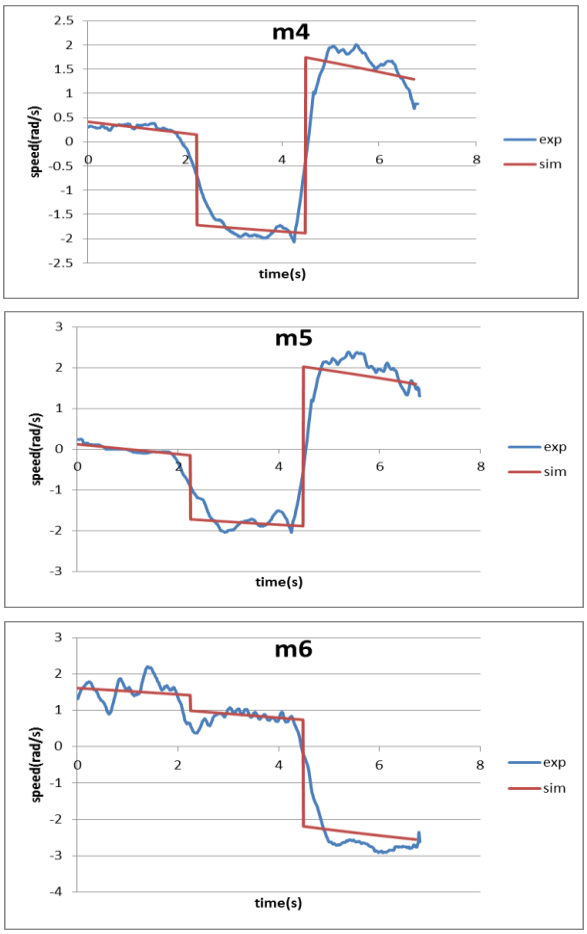

Fig. 16 Comparing the angular velocity of the motors between simulation and experimental results of Cartesian space controller

C. *Point to Point Test*

For the second case, a regulation process is conducted and the end-effector is supposed to track an optimal path between two predefined initial and final points of Eq. (26). The controlling gains are optimized here using LQR optimizer tool and an *800 gr* payload is placed on the end-effector to examine the ability of the designed regulator to neutralize the effect of parametric uncertainties.

Start point (in centimeter): *x=5, y=5, z=100*

End point (in centimeter): *x=-5, y=0, z=80* (26)

Comparison of the optimal path for simulation and experiment in which the two mentioned controlling strategies are employed is depicted here:

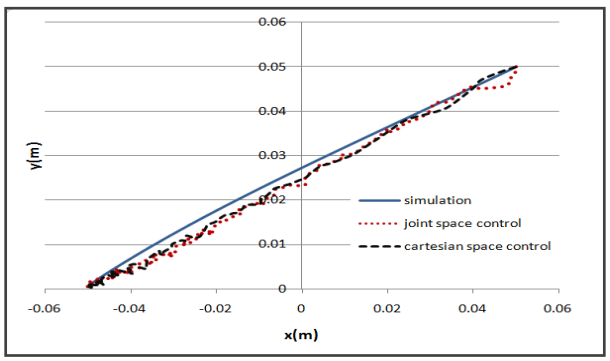

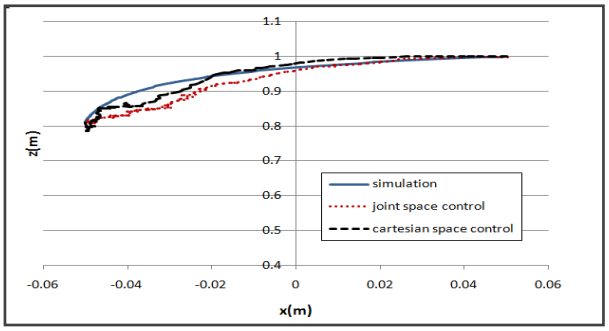

Fig. 17 Point to point path of the end- effector and its comparison between simulation and experiment

It can be seen that again here a good compatibility exists between simulation and experiment. Similar to tracking case, the system in which the actual position of the end-effector is employed for the closed loop control of the robot, results in more accurate path. The observed parabolic trend of the gained optimal path is due to LQR usage for optimizing the gains. Finally comparison of the motor speed between the simulation and the system which is equipped by Cartesian space controller is shown in Fig. 18:

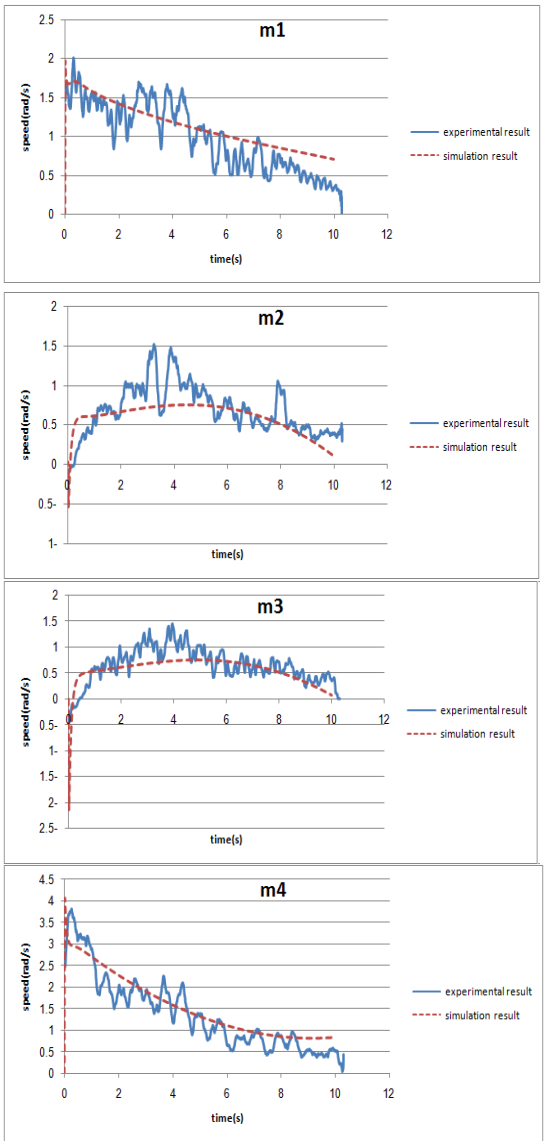

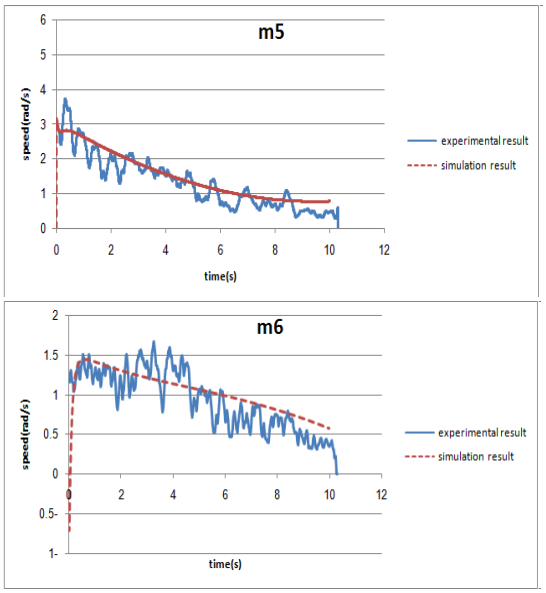

Fig. 18 Comparing the simulation and experiment of angular velocity of motors for point to point motion

It can be observed that the encoders show the result similar to simulation profile which decreases parabolic again as the result of optimal regulation. The little delay which is observed between the first moments of simulation and experiment regulation is related to high inertia and friction of the motor which prevents the angular speed to be accelerated at the initial moments of regulation like the simulation results. The vibrating response of experiment which was explained for tracking case can be observed here too which is more severe in this case because of existence of extra load as the parametric uncertainty. So the controlling strategy has to tolerate more vibrations in order to improve the path. Finally it is concluded here that as it was expected generally the norm of error for the regulation process is less than tracking. This phenomenon is related to regulatory nature of the point to point movement in which the steady state error is less than tracking. Therefore, the difference of accuracy between joint space and Cartesian space is more critical in tracking rather that regulation which is observable through the results.

VI. CONCLUSION

In this paper a new sensor fusion method is proposed for measuring all of the DOFs of the end-effector of a cable robot including translational and rotational movement in an online way.This device can be employed for every environmental situation and is able to cover whole the workspace of the robot. The output of this device is then used as the actual position in the closed loop control of the robot in order to increase its tracking accuracy. In this method the altitude of the end-effector and its rotational angle is estimated using three measurement lasers while the planar displacement is evaluated using camera and image processing. Each sensor needs to be calibrated separately and the final actual position and orientation should be calculated using the online mixture of both the mentioned sensors and employing sensor data fusion technique. It was seen that the most important superiority of the proposed algorithm is that it is able to cover whole the workspace since there is no limitation for the employed sensors. Moreover it was proved that it is applicable in any environmental situation with an acceptable cost since there it doesn't suffer from any sensing bug like the one which was mentioned for ultrasonic and gyroscope. The procedure of calculating the actual value of all of the end-effector DOFs was presented using the instantaneous online data of both the sensors and the required calibration process was performed. Some techniques were also presented in order to optimize the image processing and increase the speed and accuracy of measurement process. It was shown that by the aid of proposed recording algorithm of actual position and orientation of the end-effector it is possible to control the robot using the end-effector feedback and to increase the accuracy of the robot. This is possible since the amount of mathematical calculation of the proposed sensor fusion device doesn't exceed a definite range which makes it suitable for online and real time applications. The superiority and efficiency of the proposed measurement and control of the robot was then investigated by conducting some simulation and experimental study on the IUST cable robot (ICaSbot). Repeatability and accuracy of the robot was investigated by statistical analysis while the acceptable maneuverability of the end-effector was checked by conducting tracking and point to point tests of the end-effector. Comparison between the simulation and experimental results and the good compatibility proved the validity of experimental installations. Also comparison between the joint space and Cartesian space control showed the superiority of the mentioned measurement and using it in closed loop control of the robot for both the tracking and regulation process. It was seen that using the mentioned methodology decreases the error of the end-effector considerably especially in tracking (rather than regulation). It was stated that the main sources of the error of experimental tests are the high inertia and friction of the motors, structural flexibilities and the accuracy of the employed sensors and these errors are mostly compensated by the aid of proposed closed loop controller.

REFERENCES

[1] I. A. Bonev. "The true Origins of Parallel Robots", ParalleMIC: the Parallel Mechanisms Information Center, January, 2003.

[2] R. G. Roberts, T. Graham, and T. Lippitt, "On the Inverse Kinematics, Statics, and Fault Tolerance of Cable-Suspended Robots, Journal of Robotic Systems, vol. 15, pp. 581–597, 1998.

[3] J. Albus, R. Bostelman, and N. Dagalakis, "The NIST ROBOCRANE," Journal of Robotic Systems, vol. 10, no. 5, pp. 709–724, 1993.

[4] W.J. Shiang, D. Cannon, J. Gorman, "Dynamic Analysis of the Cable Array Robotic Crane", IEEE International Conference on Robotics and Automation, pp. 495-500, 1999.

[5] R. Bostelman, J. Albus, N. Dagalakis, A. Jacoff, "RoboCrane Project: An Advanced Concept for Large Scale Manufacturing", Intelligent Systems Division National Institute of Standards and Technology Gaithersburg, Maryland, 1995.

[6] A.H. Chang, "Experimental Development of the Mobile Vestibular Platform", SUNFEST Technical Report, Center for Sensor Technologies, University of Pennsylvania, Philadelphia, PA, 2004.

[7] R. L. Williams II, B. Snyder, J. Albus, and R. Bostelman, "Seven-DOF Cable-Suspended Robot with Independent Metrology", ASME Int. Des. Eng. Tech. Conf. Comp. Inf. Eng. Conf., 2004.

[8] J.H. Lee, S.J. Park, S.W. Oh, Y.S. Kim, "A Study on the Work Efficiency Improvement of Tower Crane Operation Using GPS and Machine Vision", Journal of Architectural Institute of Korea 18 (11), pp.133–140, 2002.

[9] E. Ottaviano, M. Ceccarelli, M. De Ciantis, "A 4–4 Cable-Based Parallel Manipulator for an Application in Hospital Environment," Control & Automation, MED '07. Mediterranean Conference, pp.1-6, 27-29 June 2007.

[10] L.Mejias, P.Campoy, K. Usher, J. Roberts, P.Corke, "Two Seconds to Touchdown - Vision-Based Controlled Forced Landing," Intelligent Robots and Systems, 2006 IEEE/RSJ International Conference on, pp. 3527-3532, 9-15 Oct. 2006.

[11] B.H. Kim, M.R. Song, "Semi-automation of Tower Cranes, a Study on the Development of Semi-Automatic Equipment of Construction Machinery (VI)", Korea Institute of Construction Technology, Ilsan, Korea, 1997.

[12] Lee, G., Kim, H.-H., Lee, C.-J., Ham, S.-I., Yun, S.-H., Cho, H., Kim, B.K., (...), Kim, K. "A laser-technology-based lifting-path tracking system for a robotic tower crane," Automation in Construction, 18 (7), pp. 865-874, 2009.

[13] A.B. Alp, "Cable Suspended Parallel Robots", Thesis for the Degree of Master of Science in Mechanical Engineering in University of Delaware, 2001.

[14] M.H. Korayem, H. Tourajizadeh, M. Bamdad, "Dynamic Load Carrying Capacity of Flexible Cable Suspended Robot: Robust Feedback Linearization Control Approach," Journal of Intelligent and Robotic Systems, 60, pp. 341– 363, 2010.

[15] M.H. Korayem, M. Bamdad, H. Tourajizadeh, H. Shafiee, R. M. Zehtab, A. Iranpour "Development of ICaSbot a Cable Suspended Robot with 6 DOFs", Arabian Journal for Science and Engineering, DOI 10.1007/s13369-012-0352-9, 2012.

[16] M. Slamani, A. Nubiola, I. Bonev, "Assessment of the positioning performance of an industrial robot", Industrial Robot: An International Journal, Vol. 39, Iss: 1, pp.57 – 68, 2012.